Earth and Planetary Science Letters 581 (2022) 117414

Contents lists available at ScienceDirect

Earth and Planetary Science Letters

www.elsevier.com/locate/epsl

Chlorine isotope behavior in subduction zone settings revealed by olivine-hosted melt inclusions from the Central America Volcanic Arc

A.-S. Bouvier [a,*], M.V. Portnyagin [b,c], S. Flemetakis [d], K. Hoernle [b,e], S. Klemme [d], J. Berndt [d], N.L. Mironov [c], T. John [f,*]

[a] Institut des Sciences de la Terre, Université de Lausanne, Switzerland
[b] GEOMAR Helmholtz Centre for Ocean Research, Kiel, Germany
[c] Vernadsky Institute of Geochemistry and Analytical Chemistry, Moscow, Russia
[d] Institut für Mineralogie, Universität Münster, Germany
[e] Institute for Geosciences, Kiel University, Germany
[f] Institute of Geological Sciences, Freie Universität Berlin, Germany

ARTICLE INFO

Article history:
Received 9 August 2021
Received in revised form 1 February 2022
Accepted 3 February 2022
Available online xxxx
Editor: F. Moynier

Keywords:
chlorine isotopes
olivine-hosted melt inclusions
Central America Volcanic Arc
secondary ion mass spectrometry
volatiles
subduction zone

ABSTRACT

The isotopic composition of Cl, a highly hydrophilic and incompatible element, can provide new insights into the processes of element recycling in subduction zone settings. Samples from 13 localities in Guatemala, El Salvador, Nicaragua and Costa Rica, representing a ca. 1000 km long NW-SE segment along the Central American Volcanic Arc (CAVA), were selected. Ninety-seven melt inclusions, hosted by olivine Fo_{90-70}, were measured for Cl isotope ratios and trace element concentrations. Melt inclusions from samples from Guatemala to northwest Nicaragua have a restricted range of $\delta^{37}Cl$ values (range $<$ 1‰ within a sample) with values decreasing from Santa Maria (Guatemala) to San Miguel (El Salvador), whereas melt inclusions from Nicaragua and Costa Rica display larger variation within a sample ($\delta^{37}Cl$ value range $>$1‰, up to 3.8‰) and do not show any systematic variation along the arc. For some samples, the $\delta^{37}Cl$ in the melt inclusions is shifted by up to 2‰ to higher values compared to bulk rock data from the same volcanic center, for which the extent of Cl degassing is not known. The combination of $\delta^{37}Cl$ values in melt inclusions with trace elements and the existing knowledge about the slab contributions along the arc allows us to elucidate the Cl isotope composition of different endmembers in this subduction zone. From Guatemala to northwest Nicaragua, a fluid component, originating from serpentinite, has a $\delta^{37}Cl$ value close to +0.6‰. This value, similar to lithospheric serpentinites, confirms that despite the aqueous fluid migration through the entire slab, Cl isotopes do not fractionate significantly during transport. A melt-like component, present in the southern part of the arc, has negative $\delta^{37}Cl$, possibly down to −2.5‰. This component has lower $\delta^{37}Cl$ than values of the oceanic crust but similar to sediments currently subducting beneath CAVA. Finally, a common component, most likely amphibole-bearing metasomatized mantle, is identified in samples with the highest $\delta^{37}Cl$ values (up to +3.0‰). The melting of amphibole, a mineral concentrating ^{37}Cl over ^{35}Cl, could explain the high $\delta^{37}Cl$ values. The difference between melt inclusions and bulk rock $\delta^{37}Cl$ in some volcanic centers probably results from late-stage processes such as mixing of different batches of magma at shallower levels after melt inclusions entrapment. Melt inclusions thus give a more comprehensive picture of Cl isotope systematics along the CAVA and in primitive subduction-related magmas.

1. Introduction

Melt inclusions in minerals, that are small droplets of melt trapped during crystal growth of primary magmatic minerals, provide insights into the nature of near-primary melts. Melt inclusions are hence less affected by superficial processes than bulk igneous rock samples, especially when melt inclusions are trapped in early crystallizing phenocrysts such as olivine. The analysis of melt inclusions is thus a powerful geochemical tool, especially suited for the study of volatile elements (such as water, carbon, sulfur or chlorine). Whereas some volatiles such as H_2O or CO_2 can be modified after entrapment due to diffusion through the host and/or into the vapor bubble (e.g., Bucholz et al., 2013; Gaetani et al.,

* Corresponding authors.
E-mail addresses: anne-sophie.bouvier@unil.ch (A.-S. Bouvier), timm.john@fu-berlin.de (T. John).

https://doi.org/10.1016/j.epsl.2022.117414

2012; Moore et al., 2015), the Cl content is unlikely to be modified (e.g., Le Voyer et al., 2014). Measurements of volatiles, coupled with other geochemical proxies (e.g., trace elements and isotopic data), can be used to track the geochemical impact of slab fluids on the mantle wedge in subduction zones (Bouvier et al., 2019; Freundt et al., 2014; Portnyagin et al., 2007; Sadofsky et al., 2008). Despite the large number of geochemical and geophysical studies on arcs, the nature and origin of the fluids escaping from the slab are still not well constrained and it is not fully understood how these fluids interact with the mantle wedge (e.g., Chen et al., 2019; Codillo et al., 2018; John et al., 2012). Amongst the different major volatiles (H_2O, CO_2, S and Cl), Cl with its two stable isotopes can be seen as the most reliable geochemical tracer, since Cl degasses at lower pressure than the other three major volatiles (e.g., Spilliaert et al., 2006). Also, Cl isotopes are not always affected by degassing: Sharp et al. (2010) suggested that only near surface degassing could fractionate Cl isotopes. However, Fortin et al. (2017) suggested that there might be some Cl isotope fractionation induced by kinetic diffusion in the growing bubble during degassing. Recently, Cl isotopes have been used to trace the Cl input into the mantle wedge (Barnes et al., 2009; Barnes and Straub, 2010; Bouvier et al., 2019; Layne et al., 2009; Manzini et al., 2017). In-situ measurements of Cl isotopes in melt inclusions can identify undegassed δ^{37}Cl signatures, which may differ from bulk rocks and thus provide new information about the Cl source(s) (Bouvier et al., 2019). So far, only three studies using SIMS reported δ^{37}Cl in-situ in melt inclusions from island arcs and back-arc settings (Bouvier et al., 2019; Layne et al., 2009; Manzini et al., 2017). In this study, we investigated the δ^{37}Cl signature in olivine-hosted melt inclusions from the Central America Volcanic Arc (CAVA). CAVA is a particularly well studied volcanic belt in terms of volcanology, geochemistry, and geophysics (Barnes et al., 2009; Carr et al., 2003; Freundt et al., 2014; Gazel et al., 2011, 2009; Heydolph et al., 2012; Hoernle et al., 2008; MacKenzie et al., 2010; Patino et al., 2000; Protti et al., 1994; Rüpke et al., 2002; Sadofsky et al., 2008; Tonarini et al., 2007; Wehrmann et al., 2014). Moreover, Cl isotopes have been measured in bulk rocks along CAVA and show values ranging from −3 to +3‰, a range larger than the δ^{37}Cl range for sediments and serpentinites reported for CAVA (Barnes et al., 2009; Barnes and Cisneros, 2012; Barnes and Sharp, 2006). The δ^{37}Cl variation is larger in the southern portion of the arc, with the most extreme positive values (>2‰) measured only in Costa Rican samples. The δ^{37}Cl values > 2‰ were interpreted as the signature of eroded high-δ^{37}Cl serpentinite fore-arc material (from Santa Elena Peninsula) incorporated into the mantle wedge (Barnes et al., 2009). The negative δ^{37}Cl values, as well as the slightly positive δ^{37}Cl (<2‰), might instead record the influence of a sediment and/or lithospheric, low-δ^{37}Cl, serpentinite-derived component. This study thus pointed out at least 2 end-members (serpentinite and sediments) with significantly different δ^{37}Cl, having a different influence along the arc. However, there remain questions about the variability of δ^{37}Cl within a small geographic area (i.e., different amounts of fluids from the same Cl source or variable influence of different Cl sources), as well as the significance of the larger δ^{37}Cl variation measured in bulk rocks compared to the CAVA Cl reservoirs (mostly sediments and serpentinites). Indeed, the last point suggests that there might be some Cl fractionation during dehydration or percolation. However, whereas intense fluid-rock interaction associated with amphibole formation may lead to significant changes in the δ^{37}Cl values (e.g., Kusebauch et al., 2015), direct evidence for slab dehydration related Cl-isotope fractionation is lacking so far (e.g., John et al., 2011).

Because of the extensive knowledge of this volcanic arc and the published bulk rock δ^{37}Cl data, CAVA is perfectly suited to improve our understanding of the behavior of Cl and Cl isotopes during subduction zone slab-to-mantle wedge transport and crustal recycling processes. In this study, we measured δ^{37}Cl in melt inclusions from 13 volcanic centers located along a northwest-southeast profile along the CAVA. The new in situ δ^{37}Cl values of the olivine-hosted melt inclusions, coupled with trace elements and δ^{37}Cl bulk rocks measured in CAVA (Barnes et al., 2009) - the first melt inclusion dataset of this kind -, can thus be used to better understand the Cl isotope behavior in subduction zone settings in the light of our current knowledge on this arc.

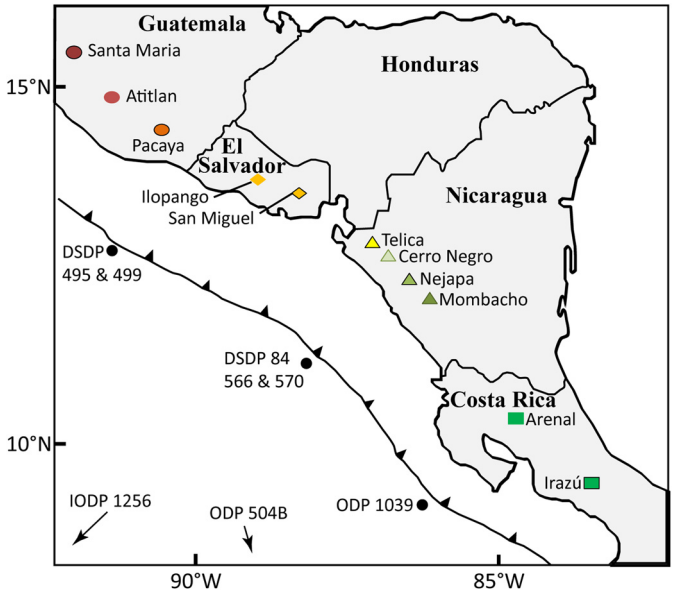

Fig. 1. Schematic map of the Central American Volcanic Arc (CAVA), modified from Sadofsky et al. (2008). The 13 volcanic centers studied here are represented using the same symbols and color code as in the following figures.

2. Geological settings and selected samples

2.1. General background

The Central America Volcanic Arc (CAVA) results from the subduction of the Cocos plate beneath the Caribbean Plate. The angle of dip of the subducting slab steepens from ∼50° beneath Guatemala and El Salvador, to 65-70° beneath Nicaragua and northern Costa Rica (MacKenzie et al., 2010; Protti et al., 1994). Crustal thickness also varies along the arc, with thinner crust beneath Nicaragua (∼35 km), and thicker crust beneath Guatemala (∼50 km) and Costa Rica (∼45 km) (e.g., Carr et al., 2003). The composition of subducted sediments is constrained by DSDP and ODP sites on the incoming plate in the northern and southern parts of the arc (Fig. 1). The sites show similar sequences of subducting sediments: hemipelagic sediments overlying pelagic carbonates, but with a larger proportion of siliceous hemipelagic sediments in the ODP Leg 170 Site1039 (up to 70% of the leg), compared to the DSDP Leg 67 Sites 495 and 499 (roughly same proportion of siliceous and carbonate sediments; e.g., Kimura et al., 1997; Plank and Langmuir, 1998).

The mantle wedge beneath CAVA has been suggested to contain depleted MORB mantle (DMM) and enriched-DMM (E-DMM) components (e.g., Carr et al., 1990; Gazel et al., 2009). Moreover, from Nicaragua to Guatemala there is an increasing contribution from an enriched component, which is not detected further south. Heydolph et al. (2012) proposed that this component could be a pyroxenitic component located in the lithospheric mantle beneath Guatemala and possibly El Salvador.

Different slab components have been identified along the arc based on geochemical tracers (e.g., fluid mobile/fluid immobile el-

Table 1
Summary of the δ^{37}Cl published values for different endmembers for CAVA. See Fig. 1 for location of drill sites.

Potential source of Cl	Sites	Location	$\delta^{37}Cl_{WSC}$	$\delta^{37}Cl_{SBC}$	Bulk δ^{37}Cl	*n*	Refs.
Sediments							
	DSDP Leg 67 Sites 495 and 499	coast of Guatemala	−0.5 to +0.2‰ (−0.2‰)	−0.8 to +0.7‰ (−0.1‰)	−0.5 to −0.1‰ (−0.3‰)	5	[1]
	ODP Leg 170 Site 1039	coast of Costa Rica	+0.1 to +0.5‰ (+0.3‰)	−2. 0 to +0.7‰ (−0.6‰)	+0.1 to +0.5‰ (+0.4‰)	7	[1]
Altered Oceanic Crust							
	IODP Site 1256D	Cocos Plate	*n.d.*	*n.d.*	−0.2 to +1.3‰ (+0.2‰)	10	[2]
	ODP Site 504B	Costa Rican rift	*n.d.*	*n.d.*	−0.4 to +1.2‰ (+0.2‰)	16	[2]
Serpentinites							
	DSDP Leg 84 Site 566	coast of Guatemala	+0.2 to +0.3‰ (+0.2‰)	+0.2 to +1.2‰ (+0.7‰)	+0.3 to +0.4‰ (+0.4‰)	2	[3]
	DSDP Leg 84 Site 570	coast of Guatemala	−0.7 to −0.3‰ (−0.5‰)	−0.5 to −0.5‰ (−0.5‰)	−0.4 to −0.7‰ (−0.5‰)	3	[3]

Numbers in parentheses are the mean values. *n.d.*: not determined. WSC: water soluble chlorine; SBC: structurally bounded chlorine. Bulk $\delta^{37}Cl = [(X\ Cl_{WSC})(\delta^{37}Cl_{WSC}) + (X\ Cl_{SBC})(\delta^{37}Cl_{SBC})$. References (Refs.): [1] Barnes et al. (2009), [2] Barnes and Cisneros (2012), [3] Barnes and Sharp (2006).

ement ratios, radiogenic isotopes, volatile element concentrations), possibly as a consequence of physical segmentation of the slab (e.g., Carr et al., 2003). The main slabs components are an aqueous fluid-like component and a melt-like component. The aqueous fluid is mainly seen in the northern part of the arc, where its relative contribution increases from Guatemala to Northern Nicaragua. The aqueous fluid is characterized by high Ba/La and B/La ratios as well as high δ^{11}B (e.g., Leeman et al., 1994; Patino et al., 2000; Tonarini et al., 2007). This fluid component with low δ^{18}O is probably derived largely from serpentinite in the down-going slab (Eiler et al., 2005; Heydolph et al., 2012; Rüpke et al., 2002; Sadofsky et al., 2008). High Ba/Th, U/La, ^{10}Be/^{9}Be and δ^{15}N indicates that the aqueous fluid also carries material from hemipelagic sediments (Eiler et al., 2005; Elkins et al., 2006; Fischer et al., 2002; Morris et al., 1990; Patino et al., 2000). A melt-like component with low Ba/La, U/Th and high La/Sm and δ^{18}O, which dominates the composition of magmas in Guatemala, is thought to represent a melt derived from metasomatized lithospheric mantle beneath the northern part of the arc (Heydolph et al., 2012).

In Costa Rica, volcanic gases exhibit δ^{15}N values typical of mantle values (Fischer et al., 2002), and bulk rocks have Ba/La, Th/U (Carr et al., 1990; Patino et al., 2000) and δ^{18}O in olivine phenocrysts (Eiler et al., 2005) similar to mantle values, suggesting only limited impact of slab-derived fluids (<0.4%). On the other hand, it has been proposed that the trace element and Sr-Nd-Pb isotope compositions of lavas from Costa Rica were dominated by a melt-like component derived from altered oceanic crust of the Galapagos Seamount Province and Cocos Ridge (e.g., Gazel et al., 2009; Hoernle et al., 2008; Sadofsky et al., 2008). Benjamin et al. (2007) show that this melt-like component is rich in volatile elements, especially beneath Irazù (e.g., ∼3wt% H_2O, >2200 ppm Cl, >2500 ppm S and >1800 ppm F).

Seventeen tephra samples, proximal cinders and lapilli, originating from 13 volcanic centers located along a northwest-southeast transect of the CAVA were selected: Santa Maria, Atitlan and Pacaya in Guatemala; Ilopango and San Miguel in El Salvador; Telica, Cerro Negro, Nejapa and Mombacho in Nicaragua; and Arenal and Irazú in Costa Rica (Fig. 1). The compositions of the bulk tephras were reported by Sadofsky et al. (2008) and Heydolph et al. (2012). These samples have been selected because they contain olivine phenocrysts with naturally vitreous melt inclusions. The major and trace element compositions of melt inclusions from some of these samples were previously reported by Sadofsky et al. (2008).

2.2. Chlorine isotopes in CAVA

CAVA is unique in that offshore drill cores provide a reasonable characterization of the isotopic signature of Cl input beneath this arc, although data are limited (Table 1). The three Cl reservoirs (serpentinites, sediments and AOC) for CAVA show a more limited range of δ^{37}Cl compared to the available data for these three Cl reservoirs globally, possibly reflecting the limited number of analysis from CAVA (Table 1 and for a compilation, e.g., Bouvier el al., 2019). Chlorine isotopes in bulk rocks can be reported as δ^{37}Cl of water-soluble Cl (noted $\delta^{37}Cl_{WSC}$; Cl absorbed at the surface of minerals), δ^{37}Cl of structurally-bounded Cl ($\delta^{37}Cl_{SBC}$) and bulk δ^{37}Cl, which is the weighted average of $\delta^{37}Cl_{WSC}$ and $\delta^{37}Cl_{SBC}$. Whereas water soluble chlorine is probably lost early during dehydration of the slab, $\delta^{37}Cl_{SBC}$ is likely to represent the δ^{37}Cl of the fluids being added to the mantle wedge (Barnes et al., 2009; John et al., 2011), assuming dehydration without kinetic fractionation. CAVA sediments could have $\delta^{37}Cl_{SBC}$ as low as −2.0‰ (Table 1; Barnes et al., 2009). The serpentinite $\delta^{37}Cl_{SBC}$ varies from 0.2 to 1.2‰ for DSDP Leg 84 Hole 566 and is −0.5‰ for DSDP Leg 84 Hole 570. Only bulk δ^{37}Cl have been published for CAVA altered oceanic crust (AOC), directly comparable to $\delta^{37}Cl_{SBC}$ as the sample preparation procedure was designed to remove WSC, and show on average slightly more positive values compare to MORB and DMM (e.g., Barnes and Sharp, 2017).

Barnes et al. (2009) determined δ^{37}Cl in bulk lavas along the arc. Values display a large range (from −2.6 to +3.0‰), larger than the Cl input beneath CAVA (Fig. 2) and are more scattered in the Southern part of the arc. Barnes et al. (2009) concluded that the variation of δ^{37}Cl along CAVA is mostly related to variable influence of serpentinite and sediments.

3. Analytical methods

All melt inclusions from this study were analyzed for major elements before SIMS analysis. Major elements in melt inclusions and their host olivine, as well as Cl and S in melt inclusions, were measured using electron microprobe CAMECA SX50 and JEOL JXA8200 at GEOMAR, following the protocol described in Sadofsky et al. (2008) and Portnyagin et al. (2008).

Chlorine isotopes were measured using secondary ion mass spectrometer IMS 1280-HR at the University of Lausanne, Switzerland. The analytical protocol follows Manzini et al. (2017). Full analytical details can be found in Supplementary Material 1. In brief, the data were obtained using a Cs^+ source with electron gun to compensate charge on sample surface. The primary beam intensity was set to 3-4 nA. ^{37}Cl and ^{35}Cl were detected simultaneously on

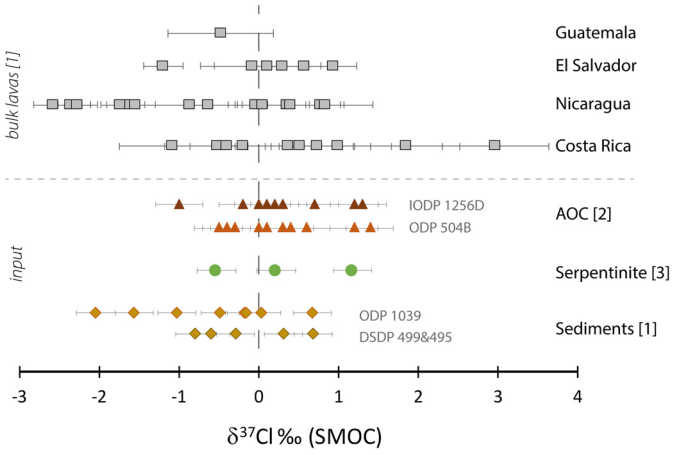

Fig. 2. Comparison of δ^{37}Cl input and output for CAVA. Chlorine isotopes for bulk lavas ([1]: Barnes et al., 2009) and AOC ([2]: Barnes and Cisneros, 2012) are bulk δ^{37}Cl – the only data available, whereas Cl isotopes reported here for serpentinite ([3]: Barnes and Sharp, 2006) and sediments ([4]: Barnes et al., 2009) are for structurally-bound chlorine, suggested to be the subducted Cl component (see text for details).

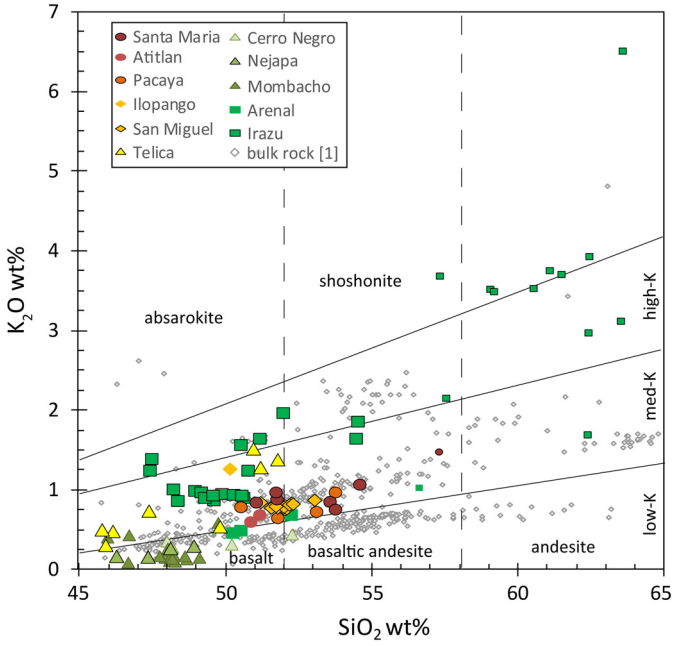

Fig. 3. SiO_2 vs. K_2O in the analyzed CAVA olivine-hosted melt inclusions. Data are corrected for post-entrapment crystallization and normalized to 100%. For comparison, CAVA bulk rocks are plotted as grey diamonds (Carr et al., 1990; Deering et al., 2012; Gazel et al., 2011, 2009; Heydolph et al., 2012; Hidalgo and Rooney, 2014; Patino et al., 2000; Wegner et al., 2011; Wehrmann et al., 2016). Here and on the following diagrams, large symbols show inclusion compositions with SiO_2 < 55 wt% and small symbols show inclusions with SiO_2 > 55 wt%. Classification from Gill (1981).

two Faraday cups (FC). Calibration was made at the beginning of each session, using 4 Cl-rich glassy reference materials (UNIL-B4, UNIL-B6, UNIL-B7, PR2) and two natural glass reference materials with low Cl content (B20-D: 336µg/g Cl and B2-1: 426 µg/g Cl; John et al., 2010; Supplementary Material 1), covering the range in major elements of the studied melt inclusions. One of the standards (B2-1 or UNIL-B4) was also inserted in each sample mount and measured regularly to check for possible mass instrumental drift. Reproducibility of the standards with Cl > 1000 µg/g was ~0.3‰ 2SD, and down to 0.8‰ 2SD for the standard with lower Cl content (down to 336 µg/g, Supplementary Material 1). The same calibration scheme as by Manzini et al. (2017) was used. Another correction was needed to correct for a bias for the low Cl content glasses (Supplementary Material 1). All raw data can be found in Supplementary Material 2a.

Trace element concentrations in large melt inclusions (>50 microns) were measured using a Thermo Fisher Scientific Element 2 sector field ICP-MS coupled to Photon Machines AnalyteG2 ArF Excimer laser system at the University of Münster, operating with a ca. 4 J/cm^2 laser fluence and a repetition rate of 10 Hz. The system was tuned with NIST SRM 612 for high sensitivity, stability, and low oxide rates (^{232}Th^{16}O/^{232}Th < 0.1%). Spot sizes for the melt inclusion analysis were between 12 and 60 µm in diameter, but in most cases 20 µm, as this proved to be the best compromise between a large enough diameter for a good signal, and a small enough diameter to avoid overlap analyses with adjacent host crystals. The signal ablation time was 40 seconds for the peak and 20 seconds for the background. Wash out time between individual spots was 10 seconds.

The NIST SRM 612 glass (Jochum et al., 2011) was used as an external standard and the BIR-1G glass (Jochum et al., 2005) as an unknown to monitor precision and accuracy (Supplementary Material 2b). Five to ten sample measurements were always bracketed by three measurements of the NIST 612 glass and two measurements of the BIR-1G glass. ^{43}Ca was used as an internal standard element, and trace element concentrations were calculated using the Glitter software (Griffin et al., 2008).

4. Results

4.1. Major and trace elements

Melt inclusions selected for this study were trapped in olivine with Fo content (Fo = 100 x Mg/(Mg+Fe)) ranging from 70 to 90, with most of them clustering around 80. The olivines with the highest Fo content (>85) were found in the southern part of the arc. Major element compositions of melt inclusions were corrected for post-entrapment crystallization, using the Petrolog software (Danyushevsky and Plechov, 2011). The compositions of melt inclusions are similar to bulk rock data from CAVA, with most melt inclusions being basaltic to basaltic andesitic, with only a few melt inclusions from the Irazù sample having andesitic compositions (Fig. 3).

Melt inclusions have trace element patterns similar to the bulk rocks from CAVA, except for B where melt inclusions often contain more B than the bulk rocks (Fig. 4). Except for a few inclusions from Nicaraguan rocks (Nejapa and Mombacho), all other melt inclusions exhibit negative Nb and positive Pb anomalies, which are typical for subduction zone magmas. The Costa Rica melt inclusions (and bulk rocks) are more enriched in incompatible trace elements compared to melt inclusions from Nicaragua, El Salvador and Guatemala. The highest Ba/La in melt inclusions and bulk rocks, which is indicative of element transfer by aqueous fluids, increases from Guatemala to northern Nicaragua and then decreases to Costa Rica (Fig. 5a; e.g., Carr et al., 1990). Contrary to Ba/La, Cl contents of melt inclusions tends to decrease from Guatemala to southern Nicaragua and increases in Costa Rica (Fig. 5b).

4.2. Chlorine isotopes

Chlorine isotope compositions of melt inclusions range from −2.1 to +3.0‰ (Fig. 5), a range four times larger than the analytical error for samples with the lowest Cl concentrations, but comparable to δ^{37}Cl data of the bulk rocks (Barnes et al., 2009). Chlorine isotopes in melt inclusions from CAVA do not display systematic variation along the arc, in contrast to Cl concentrations in melt inclusions. Chlorine isotope values of melt inclusions scatter around +1.3‰. In detail, Cl isotopes vary from one volcanic center to another, with Irazù displaying the largest internal variability.

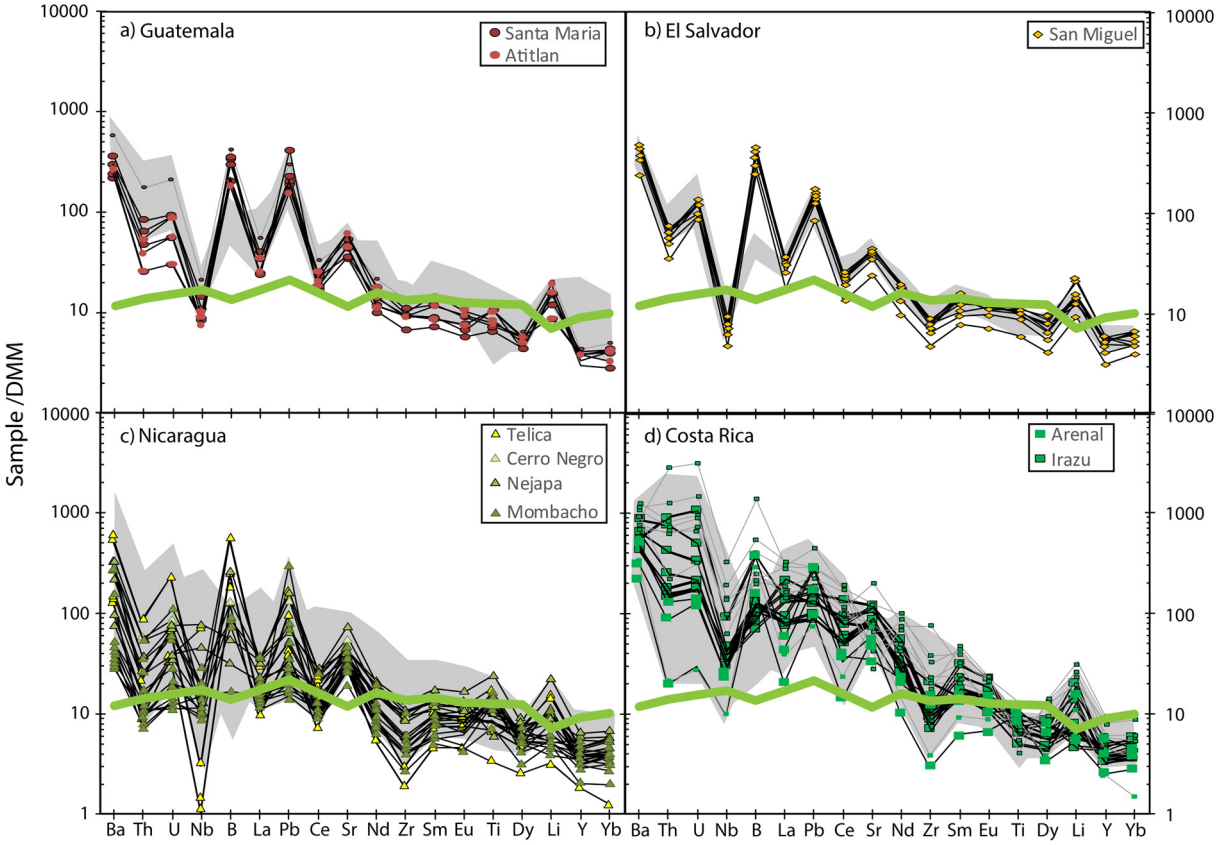

Fig. 4. Trace element concentrations of melt inclusions (symbols), normalized to depleted MORB mantle (DMM, Salters and Stracke, 2004). For comparison, the range of bulk rock data is given as the grey fields (e.g., Lloyd et al., 2013; Sadofsky et al., 2008; Wade et al., 2006; Walker et al., 2003) and the average N-MORB composition is represented by the thick light green curve (Hofmann, 1988; Marschall et al., 2017). (For interpretation of the colors in the figure(s), the reader is referred to the web version of this article.)

For four volcanic centers, melt inclusions were picked from two different samples. Different samples from a volcanic center either have averaged δ^{37}Cl with up to 1‰ difference (Arenal CR-61B and CR-61C, Cerro Negro P2-3a and P2-3b; Table 2) or are very similar (Pacaya GU-1a and GU 2a, Santa Maria GU-19d and GU-17a; Table 2). All major and trace elements and corrected δ^{37}Cl data can be found in the Supplementary Material 3.

5. Discussion

5.1. Representativeness of the studied melt inclusions

Most of the studied melt inclusions have basaltic compositions. Only 14 of 97 have basaltic andesitic or more evolved compositions. All have Cl contents similar to previously reported compositions of melt inclusions in olivine from the CAVA (e.g., Benjamin et al., 2007; Lloyd et al., 2013; Portnyagin et al., 2014; Sadofsky et al., 2008; Venugopal et al., 2016; Wade et al., 2006; Walker et al., 2003; Wehrmann et al., 2011). The similarity between trace element compositions of melt inclusions and bulk rock (Fig. 4) suggests that the selected melt inclusions do not represent boundary layers, defined as melt layer enriched in slowly diffusing elements during fast growth of the olivine host (e.g., Faure and Schiano, 2005). Indeed, diffusive fractionation in a boundary layer of a growing crystal will lead to higher δ^{37}Cl than the host melt (Fortin et al., 2017). Melt inclusions span a large range of δ^{37}Cl, as large as for CAVA bulk rocks (Barnes et al., 2009), even within a single sample, as measured for Irazù. Any analytical artefacts can be excluded to explain the observed δ^{37}Cl variability, as for the whole dataset δ^{37}Cl values correlate neither with SiO_2 nor the Cl content of melt inclusions (Fig. 6a, Supplementary Material 3). The absence of any correlation between δ^{37}Cl values and Fo content of the host olivine or SiO_2 content of the melt inclusions suggests that δ^{37}Cl variation is not linked to fractional crystallization or crustal assimilation (Fig. 6). The δ^{37}Cl values measured in melt inclusions are thus representative of the primary magmas and its variability is discussed below.

5.2. Chlorine isotope systematics within volcanoes

MORB samples, representative of the partial melting of depleted mantle without fluid addition, have between 20 and 300 ppm Cl (Michael and Cornell, 1998; Jambon et al., 1995), with the highest Cl content probably due to seawater contamination, and δ^{37}Cl of −1.0 to +0.4‰ (Sharp et al., 2013). As Cl is a very fluid mobile element (e.g., Kent et al., 2002), most melts generated in subduction zone settings have Cl content higher than MORB (i.e., from 200 to 2500 ppm, e.g., Wallace, 2005). In arc settings, the main sources of Cl input into the mantle wedge are subducting serpentinite, altered oceanic crust (AOC) and sediments (Barnes et al., 2008; John et al., 2011; Philippot et al., 1998). The studied melt inclusions have Cl contents ranging from ~300 to ~4000 ppm (Supplementary Material 3), implying that Cl has been added to the melt source to variable extents. The variable δ^{37}Cl measured both within some samples and along the arc possibly reflected the influence of different Cl sources.

As summarized in Section 2, previous studies identified a fluid and a melt component in the mantle source in the northern part of CAVA, with a maximum contribution of the fluid component in the mantle beneath northern Nicaragua (e.g., Carr et al., 2003; Heydolph et al., 2012), and a significant contribution of the melt component in the southern part of the arc (e.g., Hoernle et al.,

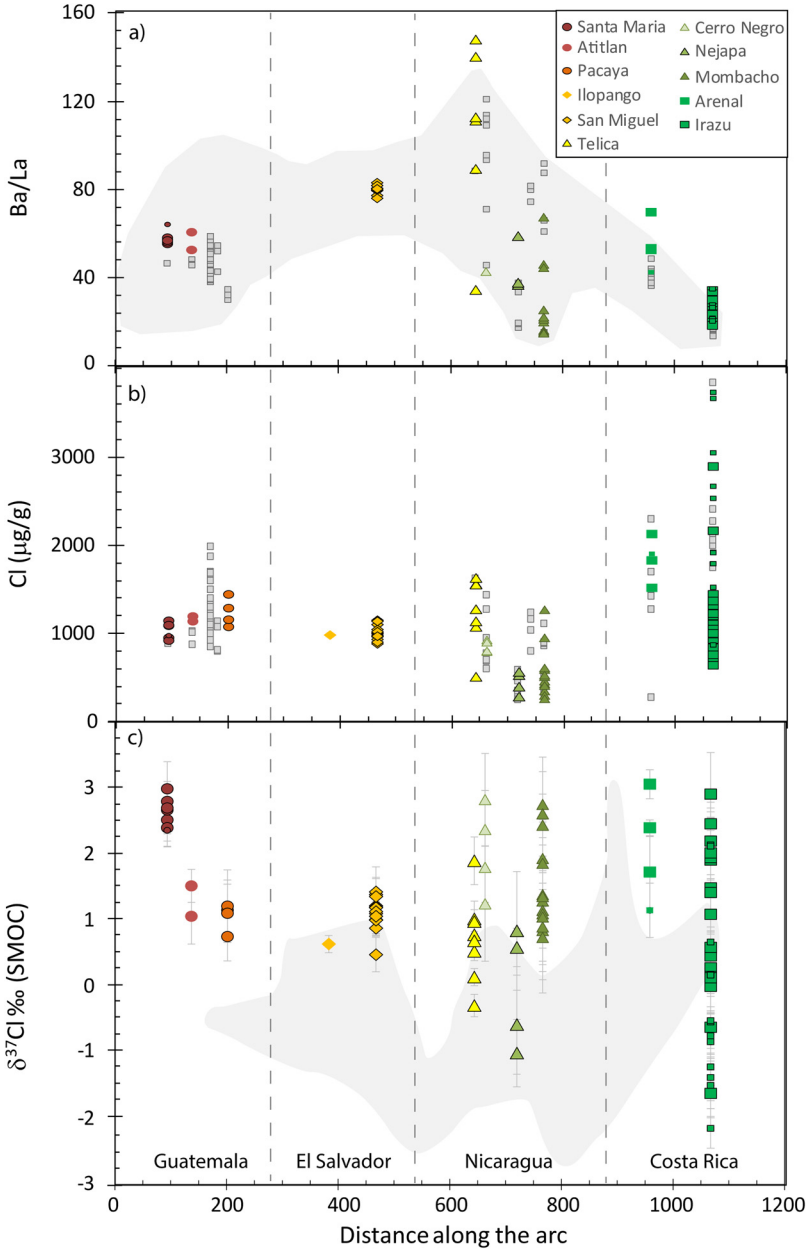

Fig. 5. Distance along the arc vs. (a) Ba/La in melt inclusions, (b) chlorine concentration and (c) chlorine isotope values. Distance along the arc is from Carr et al. (2003). Each symbol represents one melt inclusion. The grey field represents bulk rock data (d37Cl: Barnes et al., 2009; Ba/La: modified from Portnyagin et al., 2014). Grey squares represent CAVA melt inclusion data from the literature (e.g., Benjamin et al., 2007; Lloyd et al., 2013; Sadofsky et al., 2008; Wade et al., 2006; Walker et al., 2003).

Table 2
Average Cl and δ^{37}Cl for samples studied.

Volcano	Rock sample	Average Cl (µg/g)	*2sd*	Average δ^{37}Cl (‰SMOC)	*2sd*	*n*
Arenal	CR-61B	1854	*103*	1.44	*0.25*	2
	CR-61C	1807	*869*	2.73	*1.15*	2
Atitlan	GU-23b	1211	*224*	1.40	*0.26*	3
Cerro Negro	P2-3a	844	*148*	2.33	*0.76*	3
	P2-3b	887	–	1.25	–	1
Ilopango	ES20	965	–	0.64	–	1
Irazú	P2-72	1601	*1700*	0.48	*2.40*	31
Mombacho	P2-58	531	*512*	1.52	*1.40*	15
Nejapa	P2-32d	443	*232*	0.28	*1.73*	5
Pacaya	GU-1a	1103	*115*	1.18	*0.06*	2
	GU-2a	1350	*212*	0.93	*0.54*	2
San Miguel	ES29A	986	*158*	1.11	*0.46*	15
Santa Maria	GU-19d	1014	*183*	2.67	*0.51*	6
	GU-17a	1082	–	2.40	–	1
Telica	P2-16	1237	*727*	0.72	*1.28*	8

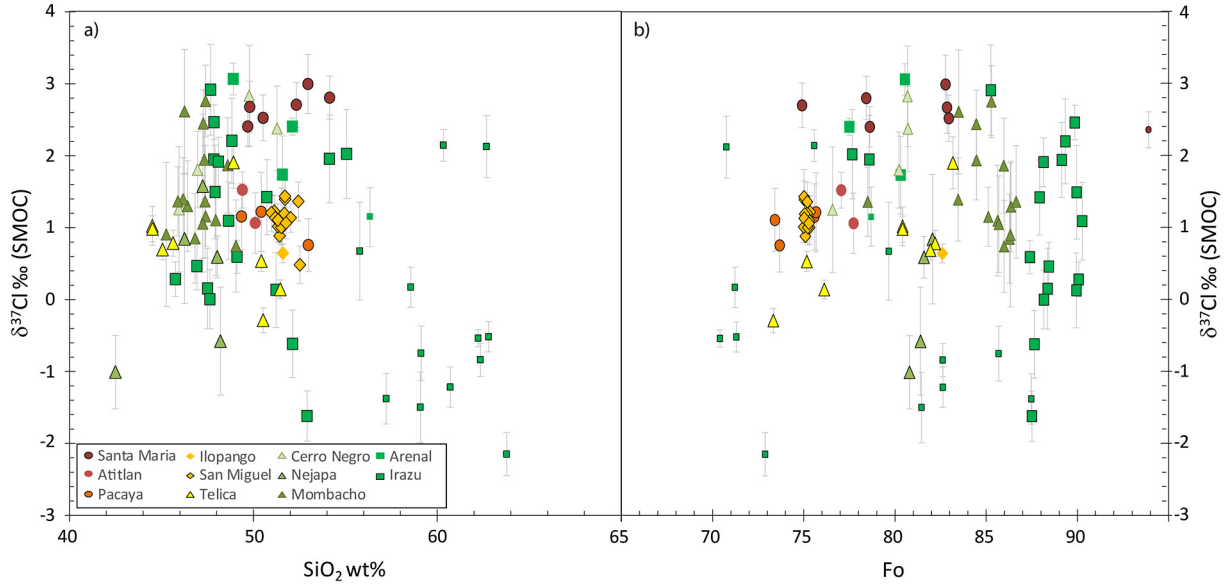

Fig. 6. Chlorine isotope values in melt inclusions compared to (a) SiO_2 (wt%) of the melt inclusions and (b) forsterite content of the host olivine (Fo). No correlation can be observed, suggesting that the Cl isotopic variation measured in the CAVA melt inclusions is not related to fractionation linked to magmatic evolution.

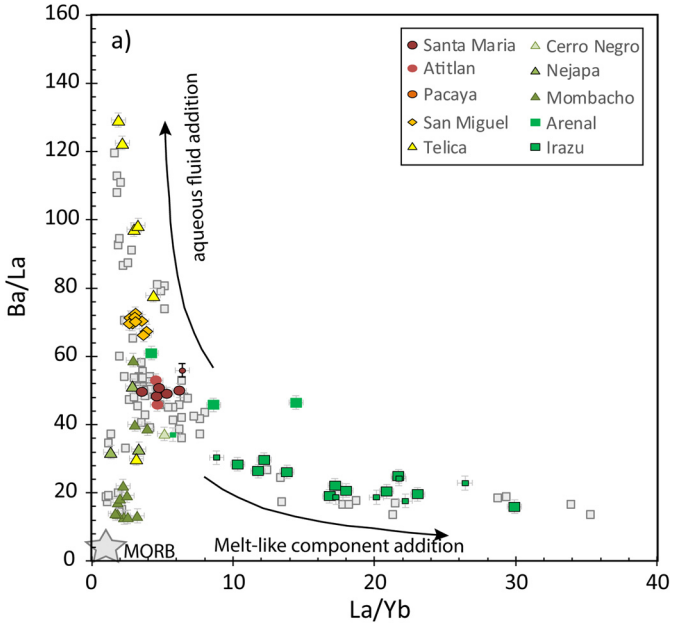

Fig. 7. Ba/La vs. La/Yb measured in melt inclusions from CAVA. Shaded grey symbols are literature data (e.g., Lloyd et al., 2013; Sadofsky et al., 2008; Wade et al., 2006; Walker et al., 2003), colored symbols are from this study. The grey star represents the composition of MORB (McDonough and Sun, 1995). All the melt inclusions have higher Ba/La than average upper mantle melts under anhydrous conditions. The melt inclusions define three trends: 1) a trend between average mantle and an aqueous fluid component, highlighted by high Ba/La, 2) melt-like components, represented by high La/Yb but low Ba/La, and 3) a trend toward the unmodified upper mantle melt composition, defined by inclusions from central Nicaragua (Mombacho and Nejapa samples).

2008). These influences can be seen for example in a plot of Ba/La (representative of aqueous fluid input, as Ba is much more fluid mobile than La) compared to La/Yb (indicative of slab melt component; Fig. 7). With these sources identified, the question remains whether influence of these two distinct sources results in different Cl concentrations and/or different δ^{37}Cl signatures of the olivine-hosted melt inclusions of our study.

The variation of Cl isotopes in melt inclusions is largest for the volcanic centers located in the southern part of the arc. This behavior is similar to that of the Cl contents and Ba/La in melt inclusions (Fig. 5 a-b) and δ^{37}Cl values in bulk rock samples (Fig. 4c; Barnes et al., 2009).

Two volcanic centers mainly defined trends toward the two different slab components (Fig. 7): Telica and Irazù. In detail, only melt inclusions from Telica show a positive relationship between δ^{37}Cl values and Fo: a 10% decrease of Fo is associated with an increase of 2.2‰ in δ^{37}Cl. However, the correlation with SiO_2 is less marked. Magmatic differentiation, which is a high temperature process, should not strongly affect δ^{37}Cl (Schauble et al., 2003). This correlation cannot result from Cl kinetic fractionation during degassing, as ^{35}Cl moves faster in the exsolving bubbles (Fortin et al., 2017). The degassed melt should thus have higher δ^{37}Cl values than the primary melt. Interestingly, δ^{37}Cl shows a crude inverse correlation with Ba/La, a tracer of element transfer in subduction zones by aqueous fluids, in the Telica melt inclusions (Fig. 8a). The highest Ba/La ratios reflect the most intense influence of an aqueous fluid component (AF), which drives the δ^{37}Cl toward lighter values.

Irazù melt inclusions display the largest δ^{37}Cl variation, but also the largest trace element variations (Fig. 4d). The more evolved melt inclusions (>58wt%) have slightly lower δ^{37}Cl (average of −0.3‰) compared to the less evolved ones (average of +0.9‰), but the range of δ^{37}Cl is relatively similar between both groups of melt inclusions (evolved: −2.2 to +2.1‰, less evolved: −1.6 to +2.9‰; Fig. 6b; Supplementary material 3), with no obvious correlation with SiO_2 or Fo with each group. Some trace element ratios such as La/Yb are also highly variable in Irazù melt inclusions (Fig. 7). The largest La/Yb variation associated with limited Ba/La variation (Fig. 7), as well as the crude negative correlation between δ^{37}Cl and La/Yb (Fig. 8b), suggests that the diversity found in δ^{37}Cl values of Irazù melt inclusions is linked to variable proportions and possibly heterogeneous δ^{37}Cl of a slab-derived melt-like component (MLC).

For the other volcanic centers, δ^{37}Cl values display no clear correlation with other geochemical tracers. Indeed, Mombacho has moderate Ba/La and low La/Yb ratios, both without clear correlation with measured δ^{37}Cl values. Melt inclusions from San Miguel and Santa Maria in northwestern CAVA display small trace-element variations associated with small variations in δ^{37}Cl values. Less than five data points are available for the other volcanic centers,

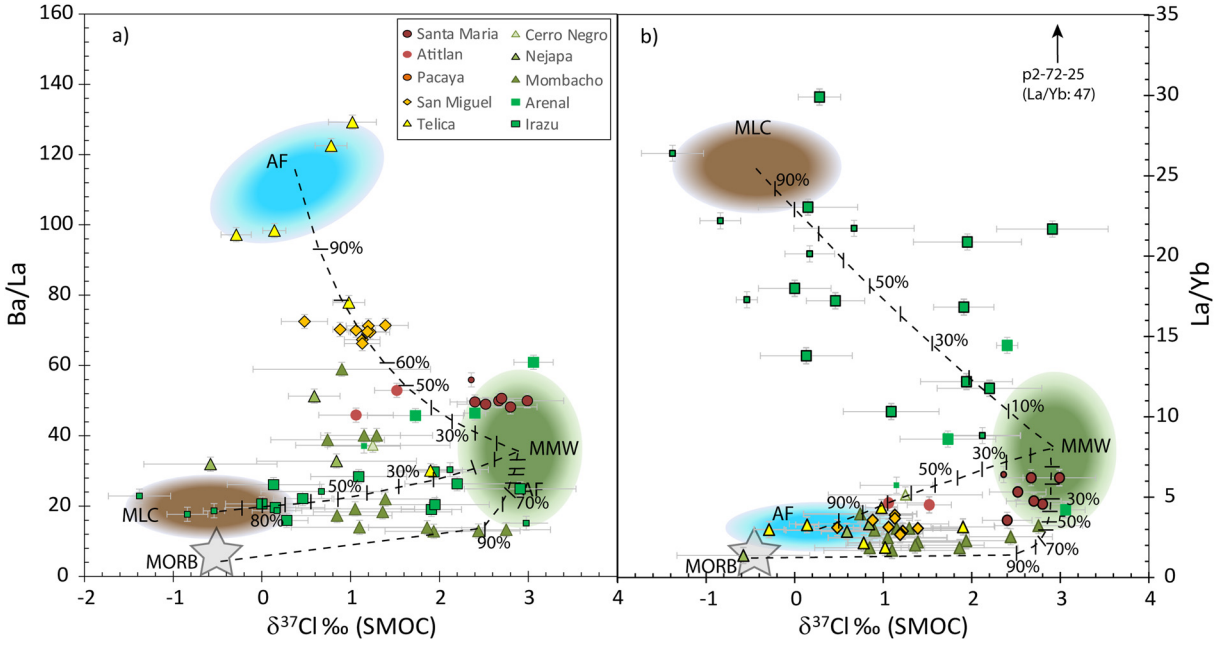

Fig. 8. Chlorine isotopes vs. (a) Ba/La and (b) La/Yb in CAVA melt inclusions. Four different endmembers, represented by ovals with graded colors, can be identified in each plot. Identification of the endmembers is discussed in the main text. Abbreviations for the four components are as follows: MMW: metasomatized-mantle wedge, AF: aqueous fluid, MLC: melt-like and unaltered (MORB) mantle melt components. MORB data for trace elements are from Hofmann (1988), and δ^{37}Cl of the mantle (unaltered peridotite) data are from Selverstone and Sharp (2011). One outlier, P2-72-25 is plotting outside Fig. 8b. Its position is indicated by an arrow. P2-72-25 is entrapped in a very evolved olivine Fo75. Its very high La/Yb and very low Sr/Ce may originate from extensive amphibole and plagioclase fractionation and are not representative of primary magma compositions.

making it difficult to clearly identify geochemical trends. Comparison of all the volcanic centers from CAVA can help constrain the origin of the variation of δ^{37}Cl in the melt inclusions and can potentially help us understand the origin of the large δ^{37}Cl variations measured in the bulk rocks.

5.3. Chlorine isotope systematics along the arc

Comparison of δ^{37}Cl values and trace-element ratios representative for slab-derived aqueous fluid input (such as Ba/La) or slab-derived hydrous melt (such as La/Yb) allows us to identify three main δ^{37}Cl melt endmembers (Fig. 8). The composition of these endmembers has been defined as an average of the composition of the most extreme melt inclusion compositions. The list of melt inclusions used to define the endmembers, as well as their compositions, can be found in Supplementary Material 4. These endmembers are thus average compositions; we acknowledge that their composition is probably more variable than as defined here.

High-Ba/La, low-La/Yb melt inclusions from Telica and low-Ba/La, high-La/Yb melts from Irazù define two melt endmembers with near-MORB δ^{37}Cl values: 1) a melt with strong imprint of an aqueous fluid from the slab (AF) and 2) a melt with influence of a melt-like component from the slab (MLC), as discussed above. The MLC is characterized by low δ^{37}Cl values (≤ -0.8‰), low Ba/La (~20) and high La/Yb ($\geq$25). The AF has high Ba/La ($\geq$105), low La/Yb (<5) and intermediate δ^{37}Cl values (~+0.6‰). Both Telica and Irazù melt inclusions also point toward a common endmember, the metasomatized mantle wedge (MMW) with high δ^{37}Cl values (~3‰), intermediate Ba/La (~36) and La/Yb (~7). San Miguel, Santa Maria and possibly also Atitlan lie on the mixing line between this common endmember (MMW) and the AF (Fig. 8). Irazù is the only volcanic center that displays a crude correlation between the MMW and the MLC. It is important to note that even though all but one Irazù melt inclusions follow a mixing trend between the MMW and the MLC, the variability around the trend shows that the MLC (and/or the MMW) has a more variable composition than the reported average composition. Nejapa and Arenal lie between the two trends, suggesting that all three endmembers play a role in the magma genesis of these volcanoes. Mombacho melt inclusions could be explained by mixing between an unmodified upper mantle melt and metasomatized mantle melt when comparing La/Yb to δ^{37}Cl (Fig. 8b). However, in detail, the most extreme melt inclusions from Mombacho plot close to MORB endmember in a plot of La/Yb compared to δ^{37}Cl, but they are enriched in Ba/La compared to MORB. This reflects the heterogeneity of MMW, which could have more variable trace element ratios, but still high δ^{37}Cl.

5.3.1. Aqueous fluid component (AF)

The involvement of an aqueous fluid component (AF) is most prominent beneath Nicaragua, as revealed by the highest fluid mobile to fluid immobile element ratios in whole rocks and in melt inclusions from Telica (e.g. Ba/La, Ba/Th, U/Th; e.g., Carr et al., 1990; Gazel et al., 2011, 2009; Heydolph et al., 2012; Patino et al., 2000; Sadofsky et al., 2008). It has been proposed that the aqueous fluids beneath CAVA most likely are derived from serpentinized slab mantle. Indeed, intense flexural faulting of the downgoing plate allows large amounts of water to enter the upper mantle and convert it to serpentinite (Ranero et al., 2003; Rüpke et al., 2002).

The Cl isotope signature of this AF (δ^{37}Cl ~ +0.6‰) is similar to the $\delta^{37}Cl_{bulk}$ or $\delta^{37}Cl_{SBC}$ measurements in CAVA serpentinites (Table 2). As John et al. (2011) have demonstrated, no Cl isotope fractionation occurs during slab dehydration. Therefore, a δ^{37}Cl of ~ +0.6‰ for an aqueous fluid originating from lithospheric serpentinite is consistent with no or only minor isotopic fractionation during fluid migration through the slab and into the mantle wedge.

Telica melt inclusions have the highest Ba/Th (up to 1800) and also relatively high, but variable, U/La (up to 0.16; Supplementary material 5), suggesting that fluids were originally derived through the deserpentinization process but picked up the trace element characteristics of carbonaceous and hemipelagic sediments during their journey into the mantle wedge. Indeed, Ba/Th and U/La have

been proposed to be good tracers of subducting carbonaceous and hemipelagic sediments beneath the CAVA (Patino et al., 2000).

5.3.2. Melt-like component (MLC)

The melt endmember with a strong imprint of a melt-like component (MLC) is characterized by δ^{37}Cl values ≤ -0.8‰ (possibly down to -2.1‰ based on Irazù's lowest melt inclusion value or even down to -2.5‰, based on bulk rocks from Concepcion (South Nicaragua); Barnes et al., 2009) and high La/Yb (>30). High La/Yb is consistent with slab melting (e.g., Gazel et al., 2011, 2009; Hoernle et al., 2008) and this is especially relevant for the southern part of CAVA (i.e., Irazù), where the Seamount Province with high La/Yb is subducting. The influence of the Seamount Province on the geochemistry of the lavas was demonstrated with radiogenic isotope data (Gazel et al., 2011, 2009; Hoernle et al., 2008).

The light δ^{37}Cl (≤ -0.8‰) of MLC is slightly lighter than the $\delta^{37}Cl_{bulk}$ of the local subducting AOC (Table 2), but similar to a few $\delta^{37}Cl_{SBC}$ measurements in sediments subducting beneath CAVA (down to -2‰; Table 1). The possible influence of subducted sediment on Cl isotopes beneath Irazù is demonstrated by crude correlations between δ^{37}Cl with Ba/Th or U/La (Supplementary Material 5). Irazù melt inclusions have the lowest Ba/Th of the melt inclusions analyzed in this study, suggesting no influence of carbonaceous sediments. On the other hand, U/La in Irazù melt inclusions are intermediate and variable. This could reflect a chemical component derived from subducted hemipelagic sediments, but our incompatible trace element and radiogenic isotope data only permit small amounts of sediment involvement (Gazel et al., 2011, 2009; Hoernle et al., 2008). Based on Barnes et al. (2009) and Barnes and Cisneros (2012) data, altered oceanic crust contains up to 40 times less Cl compared to hemipelagic sediment subducting below CAVA. Thus, even a small amount of sediment (<2%) can overprint the δ^{37}Cl signature of the subducted seawater-altered Galapagos hotspot track lavas (ocean crust).

5.3.3. The common component, metasomatized mantle wedge (MMW)

The third CAVA δ^{37}Cl melt endmember has high values ($\sim +3$‰). The δ^{37}Cl values of $\sim +3$‰ for this endmember is one of the highest δ^{37}Cl reported in any volcanic bulk rock and terrestrial Cl reservoir (Barnes and Sharp, 2017 for a review). Indeed, one value of $+3.0$‰ has been reported for Miravalles volcanic center, Costa Rica (Barnes et al., 2009) and one other of $+3.0$‰ for Pululahua volcano, Ecuador (Chiaradia et al., 2014). As this component is found in all samples, it could represent the composition of the mantle wedge. The relatively low Ba/La is a strong argument against a significant contribution of an aqueous fluid and the relatively low La/Yb rules out a major contribution from a melt-like component. An E-DMM mantle source has been suggested to be representative of the mantle wedge beneath CAVA (e.g., Gazel et al., 2009), but Ba/La of this melt component ($\sim$35) is far higher than E-MORB (Ba/La of $\sim$10; e.g., McDonough and Sun, 1995; Ulrich et al., 2012). A higher Ba/La compared to E-DMM melts suggests a component more enriched in fluid-mobile elements. Heydolph et al. (2012) suggested that pyroxenite is present in the lithosphere and perhaps also in the lower crust from Guatemala to Nicaragua. The presence of hydrous mineral in the mantle source, such as amphibole, could explain the higher Ba/La. Also, amphibole contains more Cl than olivine and pyroxene (Flemetakis et al., 2021; Kusebauch et al., 2015) and could have high δ^{37}Cl when formed during high temperatures (400-500 °C) hydrothermal alteration (Barnes and Cisneros, 2012). Assuming $\sim$800 ppm of Cl in amphibole (median content for magmatic amphiboles, e.g., Chambefort et al., 2012; Humphreys et al., 2009) and a δ^{37}Cl of $+3$‰ as defined by MMW, only 2% of amphibole in the mantle would shift the δ^{37}Cl of the mantle up to $+2.8$‰ and 17 ppm Cl (instead of $\sim$1 ppm Cl; Saal et al., 2002). The presence of amphibole could be explained by previous mantle-melt reactions or by mantle metasomatism by slab derived fluids. The high temperature implied by mantle-melt reaction will possibly not result in high δ^{37}Cl, except if the reacting melt has itself a high δ^{37}Cl signature. To the contrary, metasomatism of the upper plate mantle by slab dehydration processes might have induced formation of hydrous mineral with high δ^{37}Cl. For example, Marschall and Schumacher (2012) suggested the presence of a high pressure mélange formed on top of the slab, containing chlorite, talc and amphiboles. Dehydration of such lithologies would produce melts with compositions similar to metasomatized melt mantle wedge, enriched in volatile and fluid-mobile elements (e.g., Marschall and Schumacher, 2012).

It has to be noted that even if amphibole that has formed at 500-600 °C could have high δ^{37}Cl, there are no direct measurements yet showing that the amphibole could reach a δ^{37}Cl of up to $+3$‰. As suggested by Barnes and Sharp (2017) for altered oceanic crust, it is possible that the highest δ^{37}Cl measured here require kinetic fractionation in addition to the presence of amphibole. When and/or how the isotopic fractionation could happen remains to be determined.

5.4. Difference between δ^{37}Cl in melt inclusions and bulk rocks

For six volcanic centers, there are both bulk rock and melt inclusions δ^{37}Cl data available (Barnes et al., 2009). For San Miguel and Irazù volcanic centers, the average melt inclusion data agrees with the average bulk rock data. For Telica, Cerro Negro, Nejapa and Arenal volcanic centers, the difference between melt inclusions and average bulk rock data is as high as 2.3‰. There is no relationship between the difference $\delta^{37}Cl_{bulk\ rock}$ - $\delta^{37}Cl_{melt\ inclusion}$ and the Cl content of melt inclusions (Supplementary Material 6). Also, all the Cl-rich (Cl > 1500 ppm) reference material used for the SIMS calibration were measured at the University of Mexico, where bulk rocks from CAVA were also analyzed, implying that both labs are intercalibrated.

Chlorine kinetic fractionation during degassing cannot explain the higher δ^{37}Cl in the melt inclusions compared to whole rocks, because ^{35}Cl moves faster in the gas phase than ^{37}Cl (Fortin et al., 2017). Erupted whole rocks are usually more degassed than melt inclusions. Assuming Cl kinetic fractionation during degassing, bulk rock analyses should be shifted to higher δ^{37}Cl values compared to melt inclusions, opposite to the isotopic differences observed in this study.

The comparison between melt inclusions and bulk rocks is complicated by the fact that the sample material of the two Cl isotope studies of CAVA were not done using the identical sample set. Also, the number of analysis per volcanic samples is higher in melt inclusion than in bulk rocks, which might also cause a bias. As there is some variability in δ^{37}Cl values within individual volcanic centers (Table 2), it cannot be ruled out that the discrepancy between melt inclusion and bulk rock data is due to intra-volcano variability. This could be the case for Nejapa melt inclusions. Indeed, amongst the four volcanic centers with significant difference in δ^{37}Cl between melt inclusions and bulk rocks, Nejapa is the only one having two melt inclusions with δ^{37}Cl similar to the bulk rock.

Assuming a small range of δ^{37}Cl values of bulk rocks per volcanic center, three petrological processes can explain the lower δ^{37}Cl bulk rocks compare to melt inclusions in Telica, Cerro Negro and Arenal. First, amphibole crystallization in the shallower magma batches will preferentially decrease the relative ^{37}Cl content of the melts, resulting in lower δ^{37}Cl in the bulk rocks than in the melt inclusions which were likely trapped at greater depth. This however implies that amphibole remains in the crust. For Arenal, Beard and Borgia (1989) described amphibole-bearing magmatic enclaves that crystallized on the side wall of a mafic magma reservoir. However, as described earlier in this paper, there is no

relationship between SiO_2 or Fo of olivine and δ^{37}Cl: the most evolved melt inclusion from Arenal (basaltic andesite) has a δ^{37}Cl similar, within error, to a more primary melt inclusions from the same rock sample (Fig. 6, Supplementary Material 3, 5b).

A second possibility is late stage assimilation of magmatic hydrosaline fluids, after melt inclusion entrapment. Based on the Ranta et al. (2021) model, a brine with 16.5 wt% NaCl equivalent could have δ^{37}Cl down to $-4‰$. In that case, small amounts (<1%) of hydrosaline fluid assimilation could lower δ^{37}Cl in bulk rocks. However, magmatic hydrosaline fluid exsolution mostly happens in silicic systems (andesitic or more felsic), whereas Telica, Cerro Negro and Arenal generate basalt to basaltic andesite.

A third possible explanation is that the olivines (and hence their melt inclusions) come from different melt batches that were later mixed in a magmatic chamber (e.g., Cashman et al., 2017). The composition of the most abundant and/or Cl-richer melt batch will prevail in the final bulk rock δ^{37}Cl value. The absence of bulk rocks with similarly high δ^{37}Cl values compared to the average δ^{37}Cl value of melt inclusions in Telica, Cerro Negro, Arenal and possibly Nejapa suggest that melts from the MMW most probably mix with another melt endmember with similarly high or higher Cl content but lower δ^{37}Cl (i.e., AF or MLC) after melt inclusions entrapment. Mixing of melts with these different chemical signatures would result in a dilution of the MMW signature in the mixed melts forming the bulk rock. This interpretation implies that the melt inclusions preserve the primary melt Cl isotope signatures.

6. Conclusions

The Central America Volcanic Arc, one of the best-studied arcs, provides new constraints on the Cl isotope behavior in subduction zone settings. Our large dataset of trace element concentration and Cl isotopic data from olivine-hosted melt inclusions may be summarized as:

1. Chlorine isotopes measured in melt inclusions from different samples from the CAVA vary from -2.1 to $+3.0‰$. Melt inclusions have (on average) higher δ^{37}Cl values than δ^{37}Cl of bulk rock samples.
2. Chlorine isotopes in melt inclusions show a systematic decrease from Santa Maria to Telica. Chlorine isotopes values for the southern part of the arc are more variable.
3. Chlorine isotopes measured in melt inclusions are either variable or homogeneous within a volcanic center. The δ^{37}Cl values together with the information from trace elements suggest that the variation within a sample is not related to degassing but rather variable influence of different Cl components.
4. A melt endmember with an imprint of aqueous slab fluid (AF), with the highest influence in northern Nicaragua, has a δ^{37}Cl signature $\sim+0.6‰$. This value is not consistent with fractionation of Cl isotopes during sediment or serpentinite dehydration or during migration of the AF through the slab into mantle wedge.
5. In the southern part of the arc, especially for Irazù, samples show evidence for the involvement of a melt-like component from the slab. The δ^{37}Cl signature of this component is $\leq-0.8‰$, possibly down to $-2.5‰$, which is lower than the bulk rock values or $\delta^{37}Cl_{SBC}$ measured for the subducted AOC, but similar to subducted sediments.
6. A common component with high δ^{37}Cl values ($\sim3‰$) is identified along much of the arc, representing metasomatized mantle wedge containing amphibole. The presence of amphibole in the source can explain the higher Ba/La than enriched depleted mantle (E-DMM) melts and the high δ^{37}Cl value, due to preferential incorporation of ^{37}Cl in amphibole.
7. The high δ^{37}Cl signature of the mantle wedge recorded in melt inclusions might have been diluted in some CAVA bulk rock samples due to shallow level mixing with melt batches with lower δ^{37}Cl (i.e., AF and/or MLC).

CRediT authorship contribution statement

Bouvier A.-S.: Data acquisition, Methodology, Validation, Vizualization, Conceptualization, Writing - original draft. **Portnyagin M.V.:** Resources, Writing - review & editing. **John T.:** Conceptualization, Writing - review & editing. **Flemetakis S.:** Data acquisition, Writing - review & editing. **Hoernle K.:** Writing - review & editing. **Klemme S.:** Writing - review & editing. **Berndt J.:** Data acquisition, Writing - review & editing. **Mironov N.L.:** Sample preparation Writing - review & editing.

Declaration of competing interest

The authors declare that they have no known competing financial interests or personal relationships that could have appeared to influence the work reported in this paper.

Acknowledgements

This work was supported by SwissSIMS funds. Our thanks go to Beate Schmitte (WWU Münster) for her excellent support during the LA-ICPMS measurements. This manuscript was greatly improved by thoughtful reviews from J.D. Barnes, C.J. de Hoog and an anonymous reviewer. F. Moynier is thanked for editorial handling. Funds for sample collection and generation of background information on these samples were provided by DFG SFB574 (Volatiles and fluids in subduction zones) and the GEOMAR Helmholtz Centre core funding. TJ was funded by the Deutsche Forschungsgemeinschaft (DFG, German Research Foundation) (Project Nos. 387284271, SFB 1349). A contribution from the Vernadsky Institute funds (Budget topic # 0137-2019-0012) is acknowledged.

Appendix A. Supplementary material

Supplementary material related to this article can be found online at https://doi.org/10.1016/j.epsl.2022.117414.

References

Barnes, J.D., Cisneros, M., 2012. Mineralogical control on the chlorine isotope composition of altered oceanic crust. Chem. Geol. 326–327, 51–60. https://doi.org/10.1016/j.chemgeo.2012.07.022.

Barnes, J.D., Sharp, Z., 2006. A chlorine isotope study of DSDP/ODP serpentinized ultramafic rocks: insights into the serpentinization process. Chem. Geol. 228, 246–265. https://doi.org/10.1016/j.chemgeo.2005.10.011.

Barnes, J.D., Sharp, Z.D., 2017. Chlorine isotope geochemistry. Rev. Mineral. Geochem. 82, 345–378. https://doi.org/10.2138/rmg.2017.82.9.

Barnes, J.D., Straub, S.M., 2010. Chlorine stable isotope variations in Izu Bonin tephra: implications for serpentinite subduction. Chem. Geol. 272, 62–74. https://doi.org/10.1016/j.chemgeo.2010.02.005.

Barnes, J.D., Sharp, Z.D., Fischer, T.P., 2008. Chlorine isotope variations across the Izu-Bonin-Mariana arc. Geology 36, 883–886. https://doi.org/10.1130/G25182A.1.

Barnes, J.D., Sharp, Z.D., Fischer, T.P., Hilton, D.R., Carr, M.J., 2009. Chlorine isotope variations along the Central American volcanic front and back arc. Geochem. Geophys. Geosyst. 10, Q11S17. https://doi.org/10.1029/2009GC002587.

Beard, J.S., Borgia, A., 1989. Temporal variation of mineralogy and petrology in cognate gabbroic enclaves at Arenal volcano, Costa Rica 11.

Benjamin, E.R., Plank, T., Wade, J.A., Kelley, K.A., Hauri, E.H., Alvarado, G.E., 2007. High water contents in basaltic magmas from Irazú Volcano, Costa Rica. J. Volcanol. Geotherm. Res. 168, 68–92. https://doi.org/10.1016/j.jvolgeores.2007.08.008.

Bouvier, A.-S., Manzini, M., Rose-Koga, E.F., Nichols, A.R.L., Baumgartner, L.P., 2019. Tracing of Cl input into the sub-arc mantle through the combined analysis of B, O and Cl isotopes in melt inclusions. Earth Planet. Sci. Lett. 507, 30–39. https://doi.org/10.1016/j.epsl.2018.11.036.

Bucholz, C.E., Gaetani, G.A., Behn, M.D., Shimizu, N., 2013. Post-entrapment modification of volatiles and oxygen fugacity in olivine-hosted melt inclusions. Earth Planet. Sci. Lett. 374, 145–155.

Carr, M.J., Feigenson, M.D., Bennett, E.A., 1990. Incompatible element and isotopic evidence for tectonic control of source mixing and melt extraction along the Central American arc. Contrib. Mineral. Petrol. 105, 369–380. https://doi.org/10.1007/BF00286825.

Carr, M.J., Feigenson, M.D., Patino, L.C., Walker, J.A., 2003. Volcanism and Geochemistry in Central America: Progress and Problems. Geophys. Monogr. - Am. Geophys. Union, vol. 138, pp. 153–174.

Cashman, K.V., Sparks, R.S.J., Blundy, J.D., 2017. Vertically extensive and unstable magmatic systems: a unified view of igneous processes. Science 80, 355. https://doi.org/10.1126/science.aag3055.

Chambefort, I., Dilles, J.H., Longo, A.A., 2012. Amphibole geochemistry of the Yanacocha volcanics, Peru: evidence for diverse sources of magmatic volatiles related to gold ores. https://doi.org/10.1093/petrology/egt004.

Chen, S., Hin, R.C., John, T., Brooker, R., Bryan, B., Niu, Y., Elliott, T., 2019. Molybdenum systematics of subducted crust record reactive fluid flow from underlying slab serpentine dehydration. Nat. Commun. 10. https://doi.org/10.1038/s41467-019-12696-3.

Chiaradia, M., Barnes, J.D., Cadet-Voisin, S., 2014. Chlorine stable isotope variations across the Quaternary volcanic arc of Ecuador. Earth Planet. Sci. Lett. 396, 22–33. https://doi.org/10.1016/j.epsl.2014.03.062.

Codillo, E.A., Le Roux, V., Marschall, H.R., 2018. Arc-like magmas generated by mélange-peridotite interaction in the mantle wedge. Nat. Commun. 9. https://doi.org/10.1038/s41467-018-05313-2.

Danyushevsky, L.V., Plechov, P., 2011. Petrolog3: integrated software for modeling crystallization processes. Geochem. Geophys. Geosyst. 12. https://doi.org/10.1029/2011GC003516.

Deering, C.D., Vogel, T.A., Patino, L.C., Szymanski, D.W., Alvarado, G.E., 2012. Magmatic processes that generate chemically distinct silicic magmas in NW Costa Rica and the evolution of juvenile continental crust in oceanic arcs. Contrib. Mineral. Petrol. 163, 259–275. https://doi.org/10.1007/s00410-011-0670-z.

Eiler, J.M., Carr, M.J., Reagan, M., Stolper, E., 2005. Oxygen isotope constraints on the sources of Central American arc lavas. Geochem. Geophys. Geosyst. 6, Q07007. https://doi.org/10.1029/2004GC000804.

Elkins, L.J., Fischer, T.P., Hilton, D.R., Sharp, Z.D., McKnight, S., Walker, J., 2006. Tracing nitrogen in volcanic and geothermal volatiles from the Nicaraguan volcanic front. Geochim. Cosmochim. Acta 70, 5215–5235. https://doi.org/10.1016/j.gca.2006.07.024.

Faure, F., Schiano, P., 2005. Experimental investigation of equilibration conditions during forsterite growth and melt inclusion formation. Earth Planet. Sci. Lett. 236, 882–898. https://doi.org/10.1016/j.epsl.2005.04.050.

Fischer, T.P., Hilton, D.R., Zimmer, M.M., Shaw, A.M., Sharp, Z.D., Walker, J.A., 2002. Subduction and recycling of nitrogen along the Central American margin. Science 80 (297), 1154–1158.

Flemetakis, S., Klemme, S., Stracke, A., Genske, F., Berndt, J., Rohrbach, A., 2021. Constraining the presence of amphibole and mica in metasomatized mantle sources through halogen partitioning experiments. Lithos 380–381, 105859. https://doi.org/10.1016/j.lithos.2020.105859.

Fortin, M.-A., Watson, E.B., Stern, R., 2017. The isotope mass effect on chlorine diffusion in dacite melt, with implications for fractionation during bubble growth. Earth Planet. Sci. Lett. 480, 15–24. https://doi.org/10.1016/j.epsl.2017.09.042.

Freundt, A., Grevemeyer, I., Rabbel, W., Hansteen, T.H., Hensen, C., Wehrmann, H., Kutterolf, S., Halama, R., Frische, M., 2014. Volatile (H2O, CO2, Cl, S) budget of the Central American subduction zone. Int. J. Earth Sci. 103, 2101–2127. https://doi.org/10.1007/s00531-014-1001-1.

Gaetani, G.A., O'Leary, J.A., Shimizu, N., Bucholz, C.E., Newville, M., 2012. Rapid reequilibration of H_2O and oxygen fugacity in olivine-hosted melt inclusions. Geology 40, 915–918.

Gazel, E., Carr, M.J., Hoernle, K., Feigenson, M.D., Szymanski, D., Hauff, F., Van Den Bogaard, P., 2009. Galapagos-OIB signature in southern Central America: mantle refertilization by arc-hot spot interaction. Geochem. Geophys. Geosyst. 10. https://doi.org/10.1029/2008GC002246.

Gazel, E., Hoernle, K., Carr, M.J., Herzberg, C., Saginor, I., van den Bogaard, P., Hauff, F., Feigenson, M., Swisher, C., 2011. Plume-subduction interaction in southern Central America: mantle upwelling and slab melting. Lithos 121, 117–134. https://doi.org/10.1016/j.lithos.2010.10.008.

Gill, J.B., 1981. Orogenic Andesites and Plate Tectonics, Minerals and Rocks. Springer Berlin Heidelberg, Berlin, Heidelberg.

Griffin, W.L., Powell, W.J., Pearson, N.J., O'Reilly, S.Y., 2008. GLITTER: data reduction software for laser ablation ICP-MS. In: Laser Outstanding, Ablation ICP-MS in the Earth Sciences: Current Practices and Issues. In: Short Course Series, vol. 40. Mineralogical Association of Canada, pp. 308–311.

Heydolph, K., Hoernle, K., Hauff, F., van den Bogaard, P., Portnyagin, M., Bindeman, I., Garbe-Schönberg, D., 2012. Along and across arc geochemical variations in NW Central America: Evidence for involvement of lithospheric pyroxenite. Geochim. Cosmochim. Acta 84, 459–491. https://doi.org/10.1016/j.gca.2012.01.035.

Hidalgo, P.J., Rooney, T.O., 2014. Petrogenesis of a voluminous Quaternary adakitic volcano: the case of Baru volcano. Contrib. Mineral. Petrol. 168, 1–19. https://doi.org/10.1007/s00410-014-1011-9.

Hoernle, K., Abt, D.L., Fischer, K.M., Nichols, H., Hauff, F., Abers, G.A., Van Den Bogaard, P., Heydolph, K., Alvarado, G., Protti, M., Strauch, W., 2008. Arc-parallel flow in the mantle wedge beneath Costa Rica and Nicaragua. Nature 451, 1094–1097. https://doi.org/10.1038/nature06550.

Hofmann, A.W., 1988. Chemical differentiation of the Earth: the relationship between mantle, continental crust, and oceanic crust. Earth Planet. Sci. Lett. 90, 297–314. https://doi.org/10.1016/0012-821X(88)90132-X.

Humphreys, M.C.S., Edmonds, M., Christopher, T., Hards, V., 2009. Chlorine variations in the magma of Soufrière Hills Volcano, Montserrat: insights from Cl in hornblende and melt inclusions. Geochim. Cosmochim. Acta 73, 5693–5708. https://doi.org/10.1016/j.gca.2009.06.014.

Jambon, A., Déruelle, B., Dreibus, G., Pineau, F., 1995. Chlorine and bromine abundance in MORB: the contrasting behaviour of the Mid-Atlantic Ridge and East Pacific Rise and implications for chlorine geodynamic cycle. Chem. Geol. 126, 101–117. https://doi.org/10.1016/0009-2541(95)00112-4.

Jochum, K.P., Willbold, M., Raczek, I., Stoll, B., Herwig, K., 2005. Chemical characterisation of the USGS reference glasses GSA-1G, GSC-1G, GSD-1G, GSE-1G, BCR-2G, BHVO-2G and BIR-1G using EPMA, ID-TIMS, ID-ICP-MS and LA-ICP-MS. Geostand. Geoanal. Res. 29, 285–302. https://doi.org/10.1111/j.1751-908X.2005.tb00901.x.

Jochum, K.P., Wilson, S.A., Abouchami, W., Amini, M., Chmeleff, J., Eisenhauer, A., Hegner, E., Iaccheri, L.M., Kieffer, B., Krause, J., Mcdonough, W.F., Mertz-Kraus, R., Raczek, I., Rudnick, R.L., Scholz, D., Steinhoefel, G., Stoll, B., Stracke, A., Tonarini, S., Weis, D., Weis, U., Woodhead, J.D., 2011. GSD-1G and MPI-DING reference glasses for in situ and bulk isotopic determination. Geostand. Geoanal. Res. 35, 193–226. https://doi.org/10.1111/j.1751-908X.2010.00114.x.

John, T., Scherer, E.E., Schenk, V., Herms, P., Halama, R., Garbe-Schönberg, D., 2010. Subducted seamounts in an eclogite-facies ophiolite sequence: the Andean Raspas Complex, SW Ecuador. Contrib. Mineral. Petrol. 159, 265–284. https://doi.org/10.1007/s00410-009-0427-0.

John, T., Scambelluri, M., Frische, M., Barnes, J.D., Bach, W., 2011. Dehydration of subducting serpentinite: implications for halogen mobility in subduction zones and the deep halogen cycle. Earth Planet. Sci. Lett. 308, 65–76. https://doi.org/10.1016/j.epsl.2011.05.038.

John, T., Gussone, N., Podladchikov, Y.Y., Bebout, G.E., Dohmen, R., Halama, R., Klemd, R., Magna, T., Seitz, H.M., 2012. Volcanic arcs fed by rapid pulsed fluid flow through subducting slabs. Nat. Geosci. 5, 489–492. https://doi.org/10.1038/ngeo1482.

Kent, A.J.R., Peate, D.W., Newman, S., Stolper, E.M., Pearce, J.A., 2002. Chlorine in submarine glasses from the Lau Basin: seawater contamination and constraints on the composition of slab-derived fluids. Earth Planet. Sci. Lett. 202, 361–377. https://doi.org/10.1016/S0012-821X(02)00786-0.

Kimura, G., Silver, E.A., Blum, P., et al., 1997. Shipboard scientific party. In: Proceedings of the Ocean Drilling Program, Initial Reports, pp. 45–93.

Kusebauch, C., John, T., Barnes, J.D., Klügel, A., Austrheim, H.O., 2015. Halogen element and stable chlorine isotope fractionation caused by fluid-rock interaction (Bamble sector, SE Norway). J. Petrol. 56, 299–324. https://doi.org/10.1093/petrology/egv001.

Layne, G.D., Kent, A.J.R., Bach, W., 2009. d37Cl systematics of a backarc spreading system: the Lau Basin. Geology 37, 427–430. https://doi.org/10.1130/G25520A.1.

Leeman, W.P., Carr, M.J., Morris, J.D., 1994. Boron geochemistry of the Central American Volcanic Arc: constraints on the genesis of subduction-related magmas. Geochim. Cosmochim. Acta 58, 149–168. https://doi.org/10.1016/0016-7037(94)90453-7.

Le Voyer, M., Asimow, P.D., Mosenfelder, J.L., Guan, Y., Wallace, P., Schiano, P., Stolper, E.M., Eiler, J.M., 2014. Zonation of H_2O and F concentrations around melt inclusions in olivines. J. Petrol. 55, 685–707. https://doi.org/10.1093/petrology/egu003.

Lloyd, A.S., Plank, T., Ruprecht, P., Hauri, E.H., Rose, W., 2013. Volatile loss from melt inclusions in pyroclasts of differing sizes. Contrib. Mineral. Petrol. 165, 129–153. https://doi.org/10.1007/s00410-012-0800-2.

MacKenzie, L.S., Abers, G.A., Rondenay, S., Fischer, K.M., 2010. Imaging a steeply dipping subducting slab in Southern Central America. Earth Planet. Sci. Lett. 296, 459–468. https://doi.org/10.1016/j.epsl.2010.05.033.

Manzini, M., Bouvier, A.-S., Barnes, J.D., Bonifacie, M., Rose-Koga, E.F., Ulmer, P., Métrich, N., Bardoux, G., Williams, J., Layne, G.D., Straub, S., Baumgartner, L.P., John, T., 2017. SIMS chlorine isotope analyses in melt inclusions from arc settings. Chem. Geol. 449, 112–122. https://doi.org/10.1016/j.chemgeo.2016.12.002.

Marschall, H.R., Schumacher, J.C., 2012. Arc magmas sourced from mélange diapirs in subduction zones. Nat. Geosci. 5, 862–867. https://doi.org/10.1038/ngeo1634.

Marschall, H.R., Wanless, V.D., Shimizu, N., Pogge von Strandmann, P.A.E., Elliott, T., Monteleone, B.D., 2017. The boron and lithium isotopic composition of mid-ocean ridge basalts and the mantle. Geochim. Cosmochim. Acta. https://doi.org/10.1016/j.gca.2017.03.028. Elsevier Ltd.

McDonough, W.F., Sun, S.-s., 1995. The composition of the Earth. Chem. Geol. 120, 223–253. https://doi.org/10.1016/0009-2541(94)00140-4.

Michael, P.J., Cornell, W.C., 1998. Influence of spreading rate and magma supply on crystallization and assimilation beneath mid-ocean ridges: evidence from chlorine and major element chemistry of mid-ocean ridge basalts. J. Geophys. Res. Solid Earth 103, 18325–18356. https://doi.org/10.1029/98JB00791.

Moore, L.R., et al., 2015. Bubbles matter: an assessment of the contribution of vapor bubbles to melt inclusion volatile budgets. Am. Mineral. 100, 806–823.

Morris, J.D., Leeman, W.P., Tera, F., 1990. The subducted component in island arc lavas: constraints from Be isotopes and B–Be systematics. Nature 344, 31–36. https://doi.org/10.1038/344031a0.

Patino, L.C., Carr, M.J., Feigenson, M.D., 2000. Local and regional variations in Central American arc lavas controlled by variations in subducted sediment input. Contrib. Mineral. Petrol. 138 (3), 265–283.

Philippot, P., Agrinier, P., Scambelluri, M., 1998. Chlorine cycling during subduction of altered oceanic crust. Earth Planet. Sci. Lett. 161, 33–44.

Plank, T., Langmuir, C.H., 1998. The chemical composition of subducting sediment and its consequences for the crust and mantle. Chem. Geol. 145, 325–394.

Portnyagin, M., Hoernle, K., Plechov, P., Mironov, N., Khubunaya, S., 2007. Constraints on mantle melting and composition and nature of slab components in volcanic arcs from volatiles (H2O, S, Cl, F) and trace elements in melt inclusions from the Kamchatka Arc. Earth Planet. Sci. Lett. 255, 53–69. https://doi.org/10.1016/j.epsl.2006.12.005.

Portnyagin, M., Almeev, R., Matveev, S., Holtz, F., 2008. Experimental evidence for rapid water exchange between melt inclusions in olivine and host magma. Earth Planet. Sci. Lett. 272, 541–552. https://doi.org/10.1016/j.epsl.2008.05.020.

Portnyagin, M.V., Hoernle, K., Mironov, N.L., 2014. Contrasting compositional trends of rocks and olivine-hosted melt inclusions from Cerro Negro volcano (Central America): implications for decompression-driven fractionation of hydrous magmas. Int. J. Earth Sci. 103, 1963–1982. https://doi.org/10.1007/s00531-012-0810-3.

Protti, M., Gündel, F., McNally, K., 1994. The geometry of the Wadati—Benioffzone under southern Central America and its tectonic significance: results from a high-resolution local seismographic network. Phys. Earth Planet. Inter. 84, 271–287. https://doi.org/10.1130/SPE295-p309.

Ranero, C.R., Morgan, J.P., Mcintosh, K., Reichert, C., 2003. Bending-related faulting and mantle serpentinization at the Middle America trench. Nature 425, 367–373.

Ranta, E., Halldórsson, S.A., Barnes, J.D., Jónasson, K., Stefánsson, A., 2021. Chlorine isotope ratios record magmatic brine assimilation during rhyolite genesis. Geochem. Perspect. Lett. 16, 35–39. https://doi.org/10.7185/GEOCHEMLET.2101.

Rüpke, L.H., Morgan, J.P., Hort, M., Connolly, J.A.D., 2002. Are the regional variations in Central American arc lavas due to differing basaltic versus peridotitic slab sources of fluids? Geology 30, 1035–1038. https://doi.org/10.1130/0091-7613(2002)030<1035:ATRVIC>2.0.CO;2.

Saal, A.E., Hauri, E.H., Langmuir, C.H., Perfit, M.R., 2002. Vapour undersaturation in primitive mid-ocean-ridge basalt and the volatile content of Earth's upper mantle. Nat. Geosci. 419, 451–455.

Sadofsky, S.J., Portnyagin, M., Hoernle, K., van den Bogaard, P., 2008. Subduction cycling of volatiles and trace elements through the Central American volcanic arc: evidence from melt inclusions. Contrib. Mineral. Petrol. 155, 433–456. https://doi.org/10.1007/s00410-007-0251-3.

Salters, V.J.M., Stracke, A., 2004. Composition of the depleted mantle. Geochem. Geophys. Geosyst. 5 (5). https://doi.org/10.1029/2003GC000597.

Schauble, E.A., Rossman, G.R., Taylor Jr., H.P., 2003. Theoretical estimates of equilibrium chlorine-isotope fractionations. Geochim. Cosmochim. Acta 67, 3267–3281. https://doi.org/10.1016/S0016-7037(02)01375-3.

Selverstone, J., Sharp, Z.D., 2011. Chlorine isotope evidence for multicomponent mantle metasomatism in the Ivrea Zone. Earth Planet. Sci. Lett. 310, 429–440. https://doi.org/10.1016/j.epsl.2011.08.034.

Sharp, Z.D., Barnes, J.D., Fischer, T.P., Halick, M., 2010. An experimental determination of chlorine isotope fractionation in acid systems and applications to volcanic fumaroles. Geochim. Cosmochim. Acta 74, 264–273. https://doi.org/10.1016/j.gca.2009.09.032.

Sharp, Z.D., Mercer, J.A., Jones, R.H., Brearley, A.J., Selverstone, J., Bekker, A., Stachel, T., 2013. The chlorine isotope composition of chondrites and Earth. Geochim. Cosmochim. Acta 107, 189–204. https://doi.org/10.1016/j.gca.2013.01.003.

Spilliaert, N., Métrich, N., Allard, P., 2006. S-Cl-F degassing pattern of water-rich alkali basalt: modelling and relationship with eruption styles on Mount Etna volcano. Earth Planet. Sci. Lett. 248, 772–786. https://doi.org/10.1016/j.epsl.2006.06.031.

Tonarini, S., Agostini, S., Doglioni, C., Innocenti, F., Manetti, P., 2007. Evidence for serpentinite fluid in convergent margin systems: the example of El Salvador (Central America) arc lavas. Geochem. Geophys. Geosyst. 8, Q09014. https://doi.org/10.1029/2006GC001508.

Ulrich, M., Hémond, C., Nonnotte, P., Jochum, K.P., 2012. OIB/seamount recycling as a possible process for E-MORB genesis. Geochem. Geophys. Geosyst. 13. https://doi.org/10.1029/2012GC004078.

Venugopal, S., Moune, S., Williams-Jones, G., 2016. Investigating the subsurface connection beneath Cerro Negro volcano and the El Hoyo Complex, Nicaragua. J. Volcanol. Geotherm. Res. 325, 211–224. https://doi.org/10.1016/j.jvolgeores.2016.06.001.

Wade, J.a., Plank, T., Melson, W.G., Soto, G.J., Hauri, E.H., 2006. The volatile content of magmas from Arenal volcano, Costa Rica. J. Volcanol. Geotherm. Res. 157, 94–120. https://doi.org/10.1016/j.jvolgeores.2006.03.045.

Walker, J.A., Roggensack, K., Patino, L.C., Cameron, B.I., Matias, O., 2003. The water and trace element contents of melt inclusions across an active subduction zone. Contrib. Mineral. Petrol. 146, 62–77. https://doi.org/10.1007/s00410-003-0482-x. ST-the water and trace element contents o.

Wallace, P.J., 2005. Volatiles in subduction zone magmas: concentrations and fluxes based on melt inclusion and volcanic gas data. J. Volcanol. Geotherm. Res. 140, 217–240. https://doi.org/10.1016/j.jvolgeores.2004.07.023.

Wegner, W., Wörner, G., Harmon, R.S., Jicha, B.R., 2011. Magmatic history and evolution of the Central American Land Bridge in Panama since Cretaceous times. GSA Bull. 123, 703–724. https://doi.org/10.1130/B30109.1.

Wehrmann, H., Hoernle, K., Portnyagin, M., Wiedenbeck, M., Heydolph, K., 2011. Volcanic CO<inf>2</inf> output at the Central American subduction zone inferred from melt inclusions in olivine crystals from mafic tephras. Geochem. Geophys. Geosyst. 12, 1–16. https://doi.org/10.1029/2010GC003412.

Wehrmann, H., Hoernle, K., Jacques, G., Garbe-Schönberg, D., Schumann, K., Mahlke, J., Lara, L.E., 2014. Volatile (sulphur and chlorine), major, and trace element geochemistry of mafic to intermediate tephras from the Chilean Southern Volcanic Zone (33–43°S). Int. J. Earth Sci. 103, 1945–1962. https://doi.org/10.1007/s00531-014-1006-9.

Wehrmann, H., Freundt, A., Kutterolf, S., 2016. The 12.4 ka Upper Apoyeque Tephra, Nicaragua: stratigraphy, dispersal, composition, magma reservoir conditions and trigger of the plinian eruption. Bull. Volcanol. 78. https://doi.org/10.1007/s00445-016-1036-1.